Arch. Metall. Mater., Vol. 61 (2016), No 2, p. 503–508

DOI: 10.1515/amm-2016-0088

M. HEBDA*#, H. DĘBECKA*, K. MIERNIK*, J. KAZIOR*

SPARK PLASMA SINTERING OF LOW ALLOY STEEL MODIFIED WITH SILICON CARBIDE

The influence of adding different amounts of silicon carbide on the properties (density, transverse rupture strength, microhardness and corrosion resistance) and microstructure of low alloy steel was investigated. Samples were prepared by mechanical alloying (MA) process and sintered by spark plasma sintering (SPS) technique. After the SPS process, half of each of obtained samples was heat-treated in a vacuum furnace. The results show that the high-density materials have been achieved. Homogeneous and fine microstructure was obtained. The heat treatment that followed the SPS process resulted in an increase in the mechanical and plastic properties of samples with the addition 1wt. % of silicon carbide. The investigated compositions containing 1 wt.% of SiC had better corrosion resistance than samples with 3 wt.% of silicon carbide addition. Moreover, corrosion resistance of the samples with 1 wt.% of SiC can further be improved by applying heat treatment.

Keywords: SPS; Silicon carbide; Low-alloy steel; Mechanical alloying; Corrosion resistance.

1. Introduction

Scientific investigations have continuously been directed at improving the properties and performance of materials. Furthermore, technology development requires materials that are resistant and inexpensive. Increasing the density of sinters, which allows to obtain better mechanical properties of ready parts, is one of the most important ways of improving parts produced by Powder Metallurgy (PM) technology. Another method of enhancing the properties of sinters is by creating desired microstructures. Currently, these methods are used to improve parts made from low alloy powders, such as Astaloy [1-6]. New materials based on low-alloy steels with silicon addition are being invented. The addition of silicon allows to modify the materials' microstructures and thus improves their mechanical properties (e.g., it is possible to obtain a bainitic-austenitic microstructure). Moreover, due to the low cost of silicon powder in comparison with other conventional alloying elements in sintered steel, competitiveness of PM parts with this addition is very high. However, silicon has a high affinity for oxygen; therefore, its implementation is problematic during the sintering process of mixed powders. Mechanical alloying is the most useful process to obtain a combination of low-alloy steel with silicon carbide addition [7, 8]. Moreover, the MA process allows to homogeneously introduce silicon to low-alloy Astaloy CrL steel [9]. On the other hand, after the MA process, particles of powders are usually small and hardened; therefore, they are difficult to consolidate during the conventional method of compaction. For this reason the Spark Plasma Sintering (SPS) is more efficient than the conventional methods of powder consolidation after the MA process [10-14]. Furthermore, the addition of silicon carbide causes an increase in hardness, yield strength, elastic and creep resistance. On the other hand, if the sintering process is carried out improperly, the addition of silicon carbide may decrease impact strength and elongation, and it may significantly reduce wear resistance of sintered materials. The SPS method is a short time consolidation technique (the sintering time is shorter than in the conventional PM process and heating/cooling rates are higher), which also allows for synthesis of various materials (metals, ceramics and composites) [15-20]. Moreover, with the use of the SPS it is possible to obtain materials with a porosity below 1% which significantly increases corrosion resistance and mechanical properties. Another important factor influencing the properties of AstaloyCrL with silicon addition is the possibility of conducting heat treatment, which allows to obtain a bainitic microstructure without precipitations of carbides (which should be guaranteed by silicon addition).

The aim of the present work was to investigate the influence of adding different amounts of silicon carbide on the properties (density, transverse rupture strength, microstructure, microhardness and corrosion resistance) of Astaloy CrL sinters produced by mechanical alloying followed by the SPS process. Furthermore, the influence of the applied heat treatment on the obtained microstructure and properties of materials was investigated.

2. Materials and methods

The specimens were prepared by mechanical alloying of Astaloy CrL powders (water-atomized iron powder with the addition of 1.5 wt.% of Cr and 0.2 wt.% of Mo manufactured and supplied by Hoganas AB Sweden) with 1 wt.% of stearic acid (supplied by Sigma-Aldrich) and 1 wt.% or 3 wt.% of silicon carbide (supplied by Sigma-Aldrich). Stearic acid was added to the powder mixture as the agent controlling the mechanical alloying process and, in particular, to avoid powder

* CRACOW UNIVERSITY OF TECHNOLOGY, INSTITUTE OF MATERIALS ENGINEERING, 24 WARSZAWSKA STR., 31-155 KRAKÓW, POLAND

Corresponding author: mhebda@pk.edu.pl

particle agglomeration. The total mass of the alloyed mixture was about 80 g. For MA, a highly energetic planetary mono-ball mill (Fritsch Pulverisette 6 model) was used. The process was carried out in a tempered steel container equipped with grinding balls (Ø10 mm) under a vacuum atmosphere. The ratio of powder mass to ball mass was at a level of 1:10. The time of milling was 3 min with a 30 min intermission period, number of cycles was 100 and rotary speed 500 rot/min. Particle size for selected composition was measured by laser particle sizer Analysette 22 NanoTec (Fritsch). Carbon (0.4 wt.%, Timrex F10 PM Special Graphite supplied by TIMCAL) was added to the mixture powders directly after the MA process. The powders with added carbon were mixed using Turbula equipment for 24 h. Next, all samples were consolidated using the SPS (in the SPS HP 5 device produced by the FC company). During the process, 50 MPa pressure was applied and argon was used as a protective atmosphere. The process was carried out using 40 ms long power impulses divided by 10 ms breaks. Samples were heated at 2 °C/s to the isothermal sintering temperature of 900 °C, held at 900 °C for 10 min and then cooled at 5 °C/s to 450 °C. Annealing lasted 9 min and samples were cooled down to ambient temperature at a rate of 4 °C/s. The overall time of sample consolidation in the SPS device was 27 min. After the SPS process, cylindrical samples with a diameter of 30 mm and a height of 5 mm were obtained. Next they were cut into halves using a diamond disk in the Accutom-2 cutting machine. Half of each of the consolidated samples was heat-treated in a vacuum furnace (Seco Warwick). Samples were heated at 10 °C/s to the isothermal sintering temperature of 1200 °C, held at that temperature for 60 min and then cooled at 100 °C/s to 350 °C. Annealing lasted 180 min. Then the samples were cooled down in the furnace. Table 1 shows a summary of the samples used for the investigation. Density of the specimens was measured by the water displacement method following the ASTM B328-96 standard test method. Cuboidal 5 mm x 6 mm x 20 mm samples were used for the transverse rupture strength (TRS) test (according to ASTM B528 standards). Measurements were carried out on MTS Criterion Model 43 equipment. The metallographic investigation (cross-sections of TRS samples) was conducted using a light optical microscope (model Nexus) on specimens etched with Nital. Microstructure characterizations and microhardness (HV0.025) of samples after the SPS process as well as samples after annealing in a vacuum furnace were determined using the microhardness model Nexus 423A equipped with a Nexus Inv-1 set (at least ten measurements were carried out). Microstructures were observed also with the use of the Jeol JSM-5510LV Scanning Electron Microscope (SEM). The polarization test (using the potentiostat-galvanostat 0531 produced by the Atlas company) was carried out to determine corrosion behavior. Measurements were carried out in a three-electrode cell consisting of the specimen, a saturated calomel electrode and a platinum electrode as the working, reference and counter electrode, respectively. The electrochemical experiments were performed in 0.1 M sodium chloride solutions under atmospheric pressure and at room temperature (21 °C). Tests were carried out after 20 min of exposure of the sintered samples to ensure stabilization of the corrosion potential (E_{corr}). The exposed area of the working electrode was 7mm^2. Polarization curves were recorded between -0.85 and 0 V at a scan rate of 1 mV/s.

3. Results and discussion

Particle size distribution of commercial Astaloy CrL powder is shown in Fig. 1. Particle sizes for mixtures after mechanical alloying were also investigated. Similar results were obtained regardless of the amount of silicon carbide introduced to the mixtures. Fig. 1 also shows representative results of particle size analysis for Astaloy CrL with 3 wt.% of SiC. The median and span of particle size distributions of Astaloy CrL and Astaloy CrL with 3 wt.% of SiC after the mechanical alloying process are presented in Table 2.

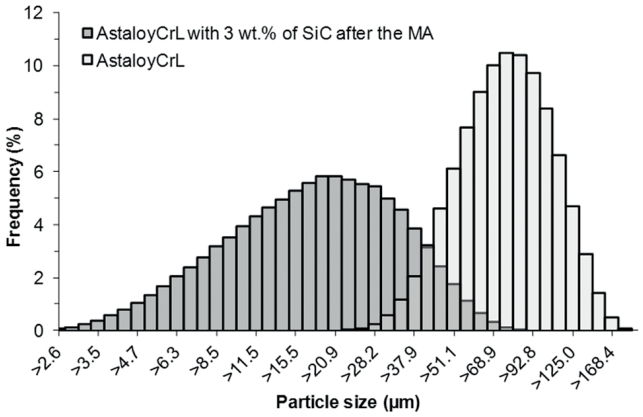

Fig. 1. Frequency of particle size distribution of commercial Astaloy CrL powder and Astaloy CrL powder with the addition of 3 wt.% of SiC after the mechanical alloying process

TABLE 1
Chemical composition and heat treatment of the tested samples

No.	Notation of samples	Chemical composition (wt.%)			Heat treatment
		Astaloy CrL	SiC	C	
1	1SiC	98.6	1	0.4	NO
2	1SiCV	98.6	1	0.4	YES
3	3SiC	96.6	3	0.4	NO
4	3SiCV	96.6	3	0.4	YES

TABLE 2
Median and span of particle size distributions of Astaloy CrL and Astaloy CrL with 3 wt.% of SiC after the mechanical alloying process

	Astaloy CrL	Astaloy CrL with 3 wt.% of SiC after the mechanical alloying process
Median (D50) (µm)	80.00 ± 1.01	19.36 ± 0.49
Span ((D90-D10)/ D50) (µm)	0.97 ± 0.07	1.81 ± 0.06

Based on the results (Fig. 1, Table 2), it was found that the applied mechanical alloying process caused significant fragmentation of the particles. Most of the particles for the base Astaloy CrL powder had an average diameter of 80.00±1.01 µm. Particle size after mechanical alloying decreased, which can be observed for Astaloy CrL with 3 wt.% of SiC composition (D50: 19.36±0.49 µm). However, the span of the

peak for powder after mechanical alloying was much wider in comparison to the non-milled powders (Table 2).

Similar results were obtained for all prepared mixtures after the mechanical alloying process. Therefore, the mechanical alloying parameters (primarily the ratio of powder mass to ball mass, milling time, size of grinding balls and rotary speed) had a significant effect on the final size of the particles obtained after the alloying process. The obtained results are in full agreement with the results obtained for similar mechanical alloyed compositions which are characterized by the same alloying model – a ductile/brittle component system [21, 22].

Densities of samples were measured in order to establish if the consolidation process was carried out successfully. Table 3 shows the obtained results. These results show very high and similar densities for all of the investigated compositions. Therefore, any differences in the measured mechanical properties and/or corrosion resistance can be caused only by structural changes of the material.

Unetched microstructure observations were made for samples produced using the SPS as well as for samples that were heat-treated in a vacuum furnace. The microstructures of samples in unetched state show a small share of porosity (rather fine, regularly shaped and evenly distributed), reference figure 2. This effect depended neither on the amount of introduced SiC nor on the heat treatment applied. These results are in accordance with the outcomes of the density measurements. Only the microstructure of sinter with 3 wt.% of SiC after heat treatment revealed precipitations/solidified liquid phase forming a characteristic network of connections crystallized along the grain boundaries. Our earlier research showed that similar effects were obtained for Astaloy CrL with the addition of 3 wt.% of SiC and 0.6 wt.% of C after cooling at 10 °C/min, consolidated in the conventional method of compaction (single-axially compaction under pressure of 600 MPa and sintering at 1200 °C), but then the solidified liquid phases were much more massive [9].

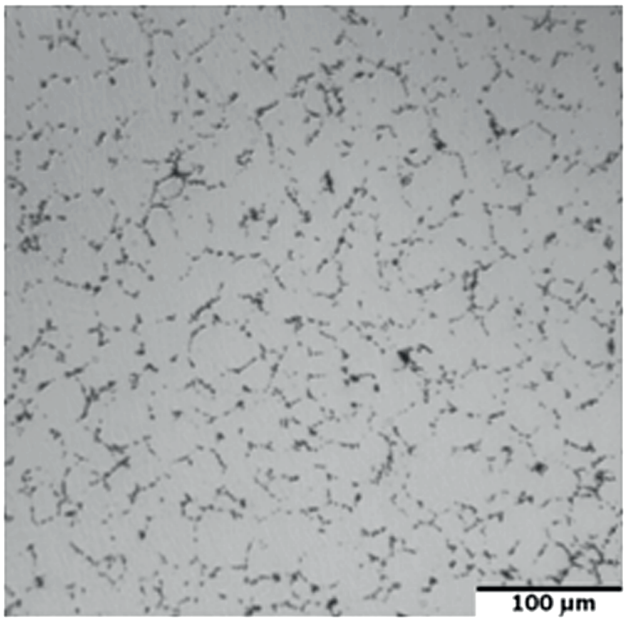

Fig. 2. Microstructure of sample processed by SPS from Astaloy CrL powder with the addition of 3 wt.% of SiC after heat treatment, unetched

Fig. 3 and 4 demonstrates the results of changes of force and displacement for all of the investigated samples recorded during the TRS test.

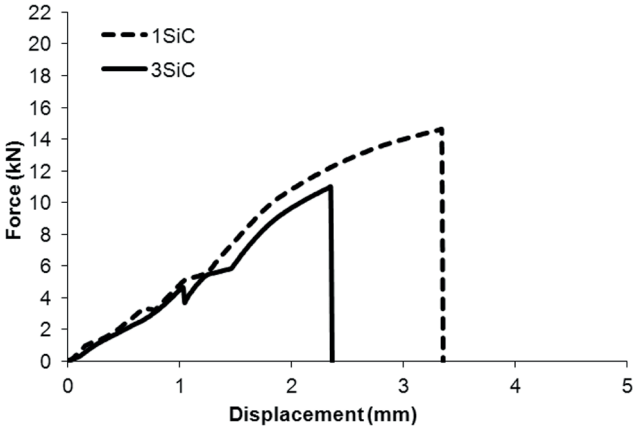

Fig. 3. Results of the TRS test for samples processed by SPS with the addition of 1 wt.% or 3 wt.% of silicon carbide before heat treatment

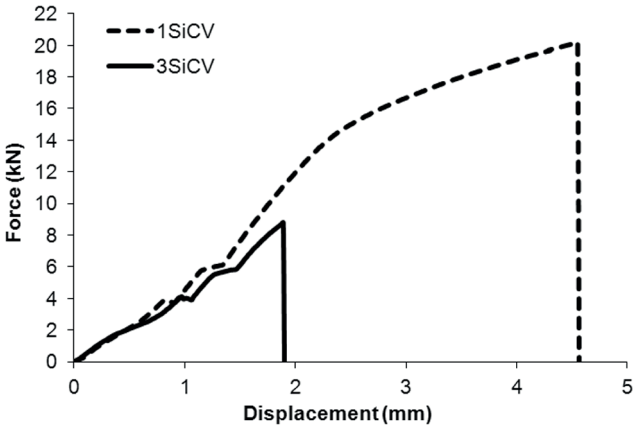

Fig. 4. Results of the TRS test for samples processed by SPS with the addition of 1 wt.% or 3 wt.% of silicon carbide after heat treatment

TABLE 3
Densities of samples processed by SPS with the addition of 1 wt.% or 3 wt.% of silicon carbide before and after heat treatment

Notation of the samples	Density (%)
1SiC	97.4 ± 0.8
1SiCV	98.1 ± 0.6
3SiC	97.2 ± 0.5
3SiCV	98.0 ± 0.4

The increase in the silicon carbide content (from 1 wt.% to 3 wt.%) caused a decrease in the strength and plastic properties of the sinters. The lower force was sufficient to destroy the sinters. Less deformation of samples before they ruptured was also recorded. Moreover, the conducted heat treatment also did not change this dependency. Better results were obtained for samples with the addition of 1 wt.% of silicon carbide introduced to the alloy. This result may indicate that SiC introduced to the base material (Astaloy CrL) can function as a finely dispersed reinforcing phase (as in the composites). Furthermore, this result may indicate that a lesser amount of reinforcement allows the heat treatment to be more effective and to achieve a better microstructure. Based on

the data obtained during the measurements (maximum force before rupture of the samples and geometric dimensions of the samples), the transverse rupture strength was calculated for all of the investigated compositions. The obtained results are presented in Table 4.

TABLE 4
Results of transverse rupture strength for samples processed by SPS with the addition of 1 wt.% or 3 wt.% of silicon carbide before and after heat treatment

Notation of samples	Transverse rupture strength (MPa)
1SiC	2355
1SiCV	2597
3SiC	2420
3SiCV	1596

TRS values for samples containing an addition of SiC were similar between the obtained results. The exception was the sample with a content of 3 wt.% of SiC after heat treatment in a vacuum furnace. Its low value of TRS (as well as a decrease of strength and plastic properties) can be explained by the visible (only for the sample obtained in this way) solidified liquid phase forming a characteristic network of connections crystallized along the grain boundaries (shown in Fig. 5).

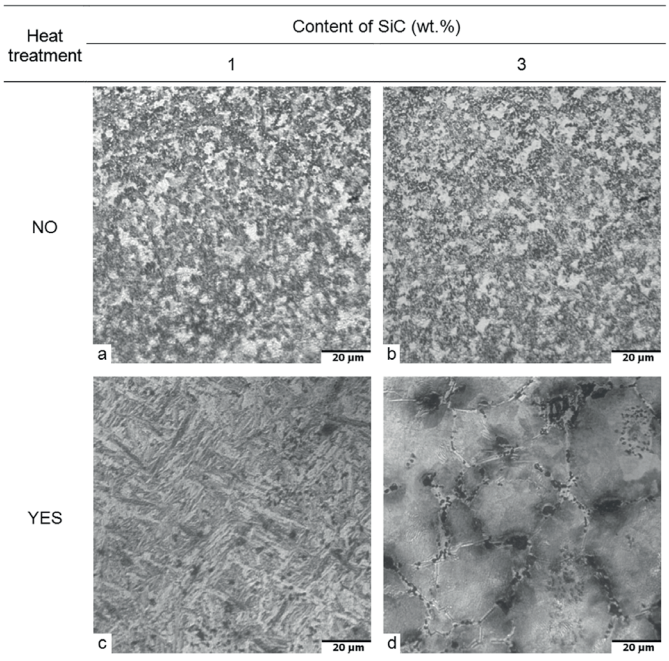

Fig. 5. Microstructures of samples processed by SPS from Astaloy CrL powder with the addition of 1 wt.% or 3 wt.% of SiC before and after heat treatment, etched

Microstructures of all investigated compositions after etching are presented in Fig. 5. For all of the investigated samples the microstructure observations revealed that the material consisted of two phases – bright and dark. These are very fine and uniformly distributed throughout the whole area of the sinters. The microstructure of the sample containing 1 wt.% of SiC after heat treatment is a typical microstructure of bainite. Introducing a higher content of SiC to the material caused crystallization of the new phase along the grain boundaries, which may be the reason for reduced mechanical properties and corrosion resistance.

The most significant changes in both the microstructures and mechanical properties were obtained for samples after heat treatment. Therefore, these microstructures were observed with the use of the SEM (Fig. 6 and 7). A comparison of microstructures of samples with the addition of silicon carbide shows that the sample with a larger amount of addition (3SiCV) has a pearlitic structure in almost the whole area. The largest grains may be observed for the sample with 3 wt.% of SiC after heat treatment. The microstructure of the sample with 1 wt.% of SiC was typical of bainite.

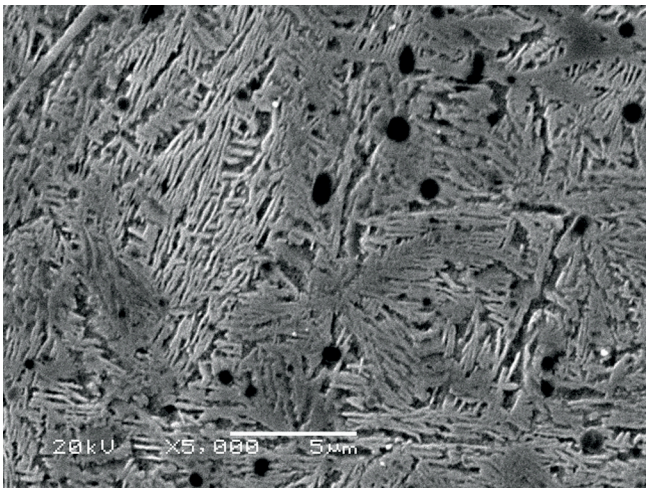

Fig. 6. Microstructure of sample processed by SPS with the addition of 1 wt.% of SiC followed by heat treatment

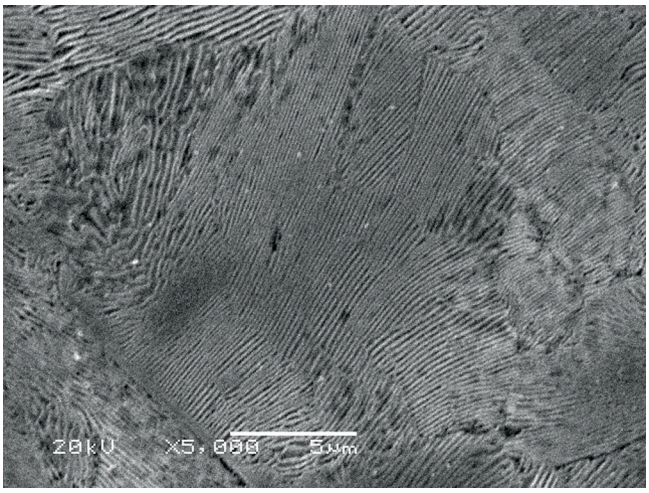

Fig. 7. Microstructure of sample processed by SPS with the addition of 3 wt.% of SiC followed by heat treatment

The manufacturer of AstaloyCrL materials states that the sintered parts, after pressing in die and conventional sintering in a furnace, have an expected value of microhardness of about 270 HV. Each of the samples with the addition of silicon carbide obtained using the SPS achieved a microhardness that was higher than 300 HV (Fig. 8). This effect is the result of having introduced the SiC addition. The increase in the silicon content increased the microhardness of the material. Moreover, a simple relation can be observed for samples with the addition of silicon carbide – heat treatment in a vacuum furnace caused an increase in microhardness (as well as

a density and TRS increase) of the samples. The largest increase was recorded for samples containing 1 wt.% of SiC addition.

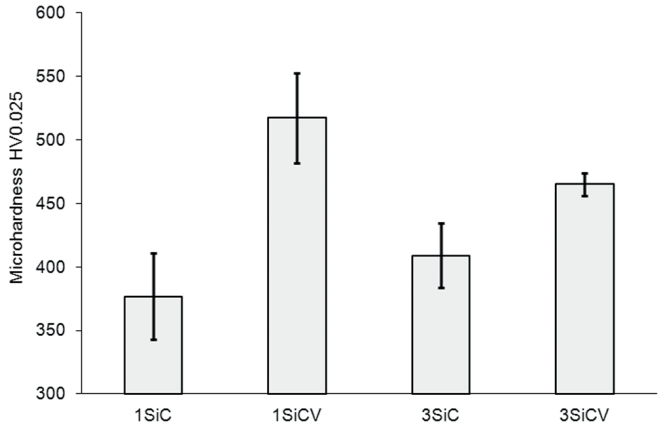

Fig. 8. Results of the microhardness test for samples processed by SPS with the addition of 1 wt.% or 3 wt.% of silicon carbide before and after heat treatment

The polarization curves (corrosion current density (log i) depending on electrode potential (E)) were determined during the corrosion test. Figures 9 and 10 present the obtained results.

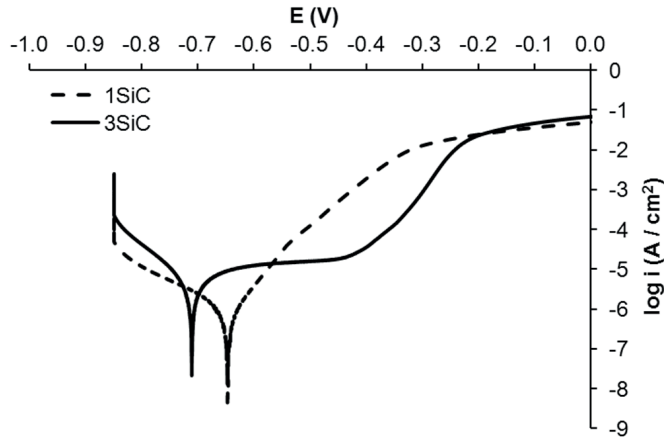

Fig. 9. Polarization curves of samples processed by SPS with the addition of 1 wt.% or 3 wt.% of silicon carbide before heat treatment

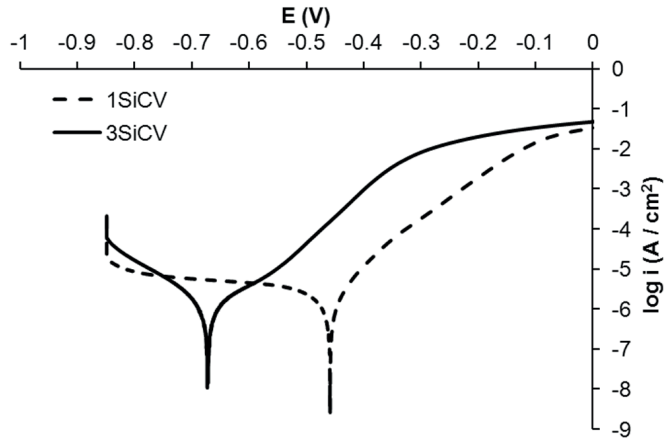

Fig. 10. Polarization curves of samples processed by SPS with the addition of 1 wt.% or 3 wt.% of silicon carbide after heat treatment

TABLE 5
Values of corrosion potential of samples processed by SPS with the addition of 1 wt.% or 3 wt.% of silicon carbide before and after heat treatment

SiC	Heat treatment	Corrosion potential E_{corr} (V)
1 (wt.%)	No	-0.710
	Yes	-0.459
3 (wt.%)	No	-0.646
	Yes	-0.672

Based on the obtained results, a corrosion potential increase after applying the heat treatment process was observed for samples containing 1 wt.% addition of SiC. This means that the samples were more resistant to corrosion. Moreover, the corrosion potential of the samples with an addition of 3 wt.% of silicon carbide is similar (before and after heat treatment). These results may be caused by the formation of the silicon-containing phase during the heat treatment process which had low corrosion resistance.

4. Conclusions

The mechanical alloying process allowed to effectively introduce silicon carbide to Astaloy CrL powder. Use of the SPS process allowed to obtain sinters from low-alloy steel with SiC addition with a density higher than 97%. All obtained materials were characterized by a fine microstructure. The heat treatment that followed the SPS process resulted in an increase in the mechanical and plastic properties of samples with the addition 1 wt.% of silicon carbide. The investigated compositions containing 1 wt.% of SiC had better corrosion resistance than samples with 3 wt.% of SiC addition. Moreover, corrosion resistance of the samples with 1 wt.% of silicon carbide can further be improved by applying heat treatment.

Acknowledgements

The work was supported by the Polish Ministry of Science and Higher Education within Grant No. NN508393237.

REFERENCES

[1] M. Teimouri, M. Ahmadi, N. Pirayesh, M. Aliofkhazraei, M. Mousavi Khoee, H. Khorsand, S. Mirzamohammadi, J. Alloys Compd. **477,** 591–595 (2009).

[2] T. Pieczonka, M. Sułowski, A. Ciaś, Archives of Metallurgy and Materials **57**(4), 1001-1009 (2012).

[3] M. Hebda, Sz. Gądek, J. Kazior, Thermal characteristics and analysis of pyrolysis effects during the mechanical alloying process of Astaloy CrM powders, Journal of Thermal Analysis and Calorimetry. **108**, 453-460 (2012).

[4] A. Ciaś, M. Sułowski, Archives of Metallurgy and Materials **54**(4), 1093-1102 (2009).

[5] L. Ciripova, E. Hryha, E. Dudrova, A. Vyrostkova, Mater. Des**. 35**, 619–625 (2012).

[6] S. Dizdar, H. Grosser, U. Engström, Wear. **273**, 17– 22 (2011).

[7] M. Azadbeh, N.P. Ahmadi, Curr. Appl. Phys. **9**, 777–782 (2009).
[8] M. Hebda, S. Gądek, M. Skałoń, J. Kazior, J Therm Anal Calorim. **113**, 395–403 (2013).
[9] M. Hebda, S. Gądek, K. Miernik, J. Kazior, Adv. Powder Technol. **25,** 543-550 (2014).
[10] J. Yi, W.J. Xue, Z.P. Xie, W. Liu, L.X. Cheng, J. Chen, H. Cheng, Y.X. Gao, Mater. Sci. Eng. A. **569,** 13–17 (2013).
[11] A. Borrell, I. Álvarez, R. Torrecillas, V.G. Rocha, A. Fernández, Mater. Sci. Eng. A. **534**, 693– 698 (2012).
[12] M.D. Unlu, G. Goller, O. Yucel and F.C. Sahin, Acta Physica Polonica. **125**(2), 257-259 (2014).
[13] K. Abdullahi, N. Al-Aqeeli, Arab. J. Sci. Eng. **39,** 3161–3168 (2014).
[14] O. Zgalat-Lozynskyy, M. Herrmann, A. Ragulya, M. Andrzejczuk, A. Polotai Archives of Metallurgy and Materials **57**(3), 853-858 (2012).
[15] T. Borkar, R. Banerjee, Mater. Sci. Eng. A. **618,** 176–181 (2014).
[16] P. Mele, H. Kamei, H. Yasumune, K. Matsumoto, K. Miyazaki, Met. Mater. Int. **20**, 389-397 (2014).
[17] S. Libardi, M. Leoni, L. Facchini, M. D'Incau, P. Scardi, A. Molinari, Mater. Sci. Eng. A. **445–446**, 244–250 (2007).
[18] M. Suśniak, J. Karwan-Baczewska, J. Dutkiewicz, M. Actis Grande, M. Rosso, Archives of Metallurgy and Materials **58**(2), 437-441 (2013).
[19] R. Yamanoglu, W. Bradbury, E.A. Olevsky, R.M. German, Met. Mater. Int. **19,** 1029-1034 (2013).
[20] G. Cipolloni, M. Pellizzari, A. Molinari, M. Hebda, M. Zadra, Powder Technol. **275**, 51-59 (2015).
[21] J.B. Fogagnolo, F. Velasco, M.H. Robert, J.M. Torralba, Mater. Sci. Eng. A**. 342,** 131–143 (2003).
[22] M. Hebda, S. Gadek, J. Kazior, Archives of Metallurgy and Materials **57**(3), 733-743 (2012).